Analysis of roller bearing cages

ROBERT KOHAR
ZBIGNIEW KRZYSIAK
MICHAL LUKAC
FRANTISEK BRUMERCIK

Robert Kohar (robert.kohar@fstroj.uniza.sk), University of Zilina, Zilina, Slovakia, Zbigniew Krzysiak (zbigniew.krzysiak@wp.pl), University of Life Sciences, Lublin, Poland; Michal Lukac (michal.lukac@fstroj.uniza.sk), University of Zilina, Zilina, Slovakia, Frantisek Brumercik (frantisek.brumercik@fstroj.uniza.sk), University of Zilina, Zilina, Slovakia.

How to cite: R. Kohar, Z. Krzysiak, M. Lukac, F. Brumercik. Analysis of roller bearing cages. Advanced Technologies in Mechanics, Vol 3, No 2(7) 2016, p. 2-11
DOI: http://dx.doi.org/10.17814/atim.2016.2(7).38

Abstract

The aim of this paper is to detail the creation of a roller bearing model with flexible body cages in the Adams program suite for subsequent dynamic analysis and to obtain information about kinematic and dynamic relationships of steel and plastic cages under various operating conditions. The bearing model was made to closely resemble its real-life counterpart, which allows us to estimate load conditions, dynamic conditions of individual bearing parts and interactions between them [1, 2].

KEYWORDS: **computer simulation, dynamic analysis, mathematical models, roller bearings**

Tapered roller bearing model

Dynamic simulations of the tapered roller bearing were performed in the MSC.Adams system. A precise geometrical model of the bearing was necessary in order to perform the said simulations. The 3D model has been created based on available drawing documentation and incorporates various methods with regards to the overall model complexity. Model design was performed in Pro/Engineer Wildfire 5 (Fig. 1), which, when compared to the MSC.Adams environment, allows simpler model creation and subsequently easier bearing geometry modifications. The bearing model assembly was transformed from Pro/Engineer into Adams environment using the Parasolid file format and was further processed based on analysis requirements [3]. The first step included material definition for individual bearing components. The bearing consisted of inner and outer ring, cage and rollers. Table 1 lists values assigned to individual parts.

Table 1. *Material properties of individual bearing parts*

	Density [kg/m^3]	Young modulus [MPa]	Poisson constant[-]
Inner ring	7850	202000	0.29
Outer ring	7850	202000	0.29
Roller	7850	202000	0.29
Steel cage	7850	202000	0.29
Plastic cage	1100	3000	0.42

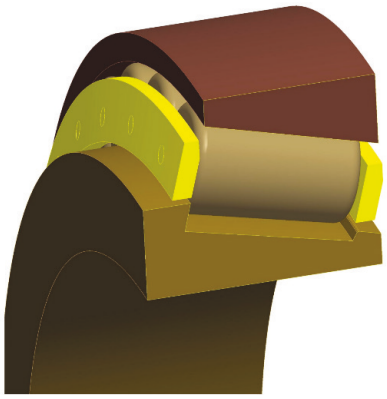

Fig. 1. *Tapered roller bearing model in Pro/Engineer*

Creation of „flexible body" cage models

Dynamic simulations of the tapered roller bearing were performed in the MSC.Adams system. Model creation along with definition of material properties, contact parameters, geometric and kinematic boundary conditions is detailed in [1]. A Modal Neutral File (MNF) file was necessary to take into account flexible properties. The said file contains important information pertaining to inertial and flexible model properties, including information necessary to integrate the flexible model within the virtual prototype in MSC.Adams program. The actual MNF file can be created in various FE programs such as Nastran, Ansys or Abaqus.

The flexible cage model was created in FE software Ansys which contains a built-in macro for this purpose. The first step consisted of finite-element mesh creation along with the definition of material properties (Fig. 2, Table 2).

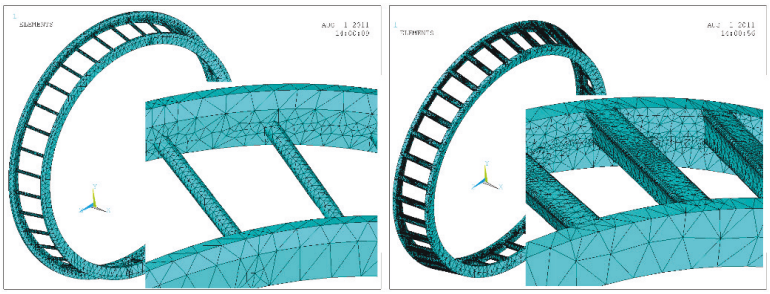

Fig. 2. *Finite-element mesh of steel (left) and plastic (right) cage in Ansys program*

Table 2. *Material properties of steel and plastic cage*

	Density [kg/m^3]	Young's modulus [Pa]	Poisson constant [-]	Element type	Number of elements
Steel cage	7850	2,02.1011	0,29	Solid 187	39105
Plastic cage	1100	3.109	0,42	Solid 187	259694

After generation of the finite-element mesh and material definition a macro is executed, creating the MNF file which requires the following user input: System of Model Units, Eigenmodes, Element Results, Shell Element Result Output Control, Filename, Solve and create export file to ADAMS.

MNF file analysis and further modification thereof is possible using the MD Adams/Flex Toolkit. The „MNF-MNF Optimizer" was used to analyze and reduce the complexity of the cage models by removing Internal Solid Element Geometry. An alternative approach is to apply the Mesh Coarsening Algorithm, resulting in reduced element counts and increased calculation speed. However, the mentioned approach also modifies node coordinates, which would invalidate load simulations obtained by dynamic simulations for further analysis in FE programs and was thus not used [4].

The next step after applying the above process consists of integration of „flex body" within MSC.Adams/View modeler. Fig. 3 shows the flexible model integration algorithm within the dynamic simulation.

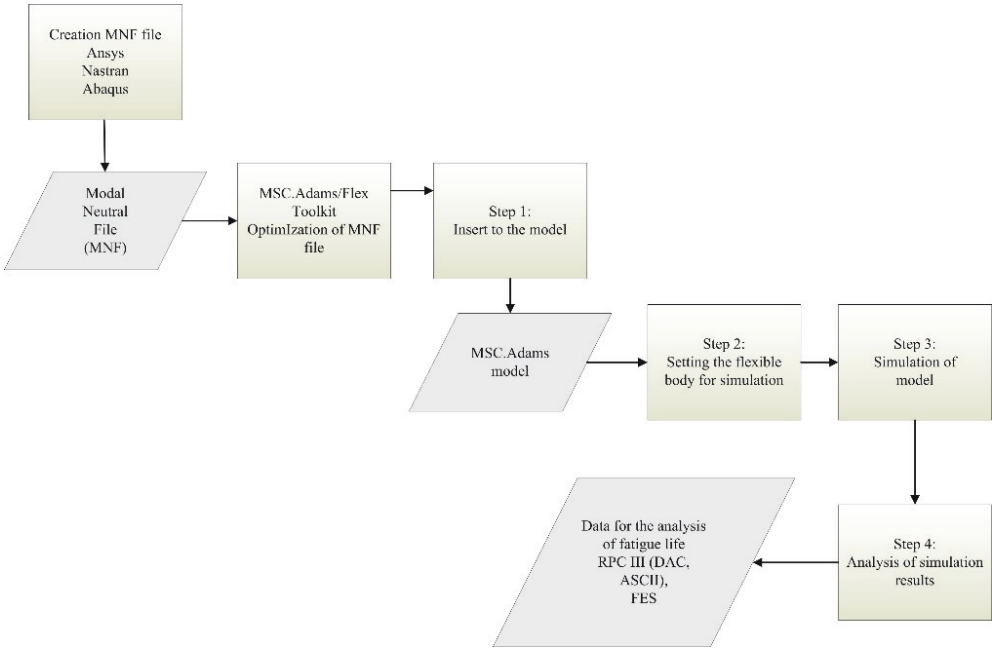

Fig. 3. *„Flexible body" integration algorithm within the dynamic simulation*

Dynamic simulation results – axial load forces Fa=518 kN with rotational speed n=15,5 min^{-1}

Dynamic simulation results with axial load force and rotational speed n = 15,5 min^{-1} represent force interactions between individual bearing parts, movement of bearing cage center of gravity and angular velocity thereof.

Fig. 4 shows a comparison of load distribution of individual rollers with theoretical calculations based on [1], wherein element load Q_{max} = 56568 N. Results of the dynamic simulation have been obtained in time t = 10 seconds.

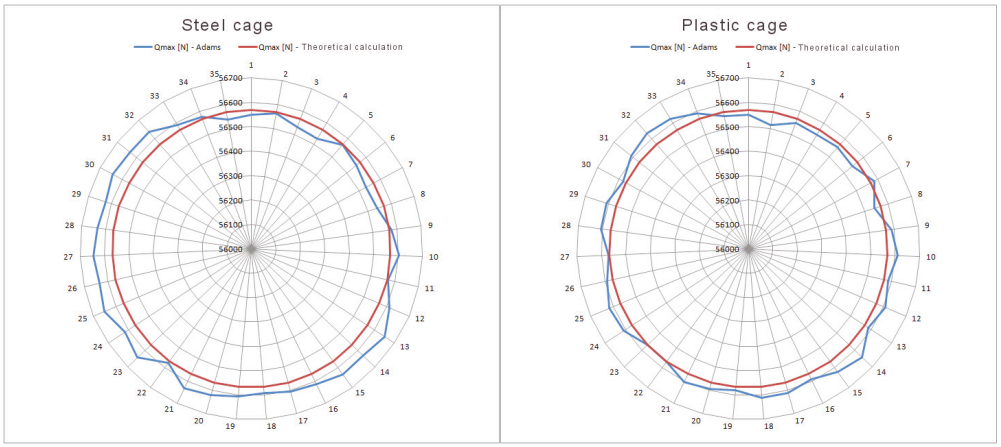

Fig. 4. *Load distribution of individual elements compared with theoretical calculations*

Figure 5 shows forces between roller and cage, roller and inner ring and angular velocity of this roller. Maximum force between steel cage and rollers was observed during interaction of the cage with roller n. 22 and is equal to 686 N (Fig. 5 up, green line). Also shown is the force between inner ring and roller n. 22 (red line), which varied between 54023 N and 58593 N. The blue line displays angular velocity of roller n. 22 and varies between 484°/s and 495°/s.

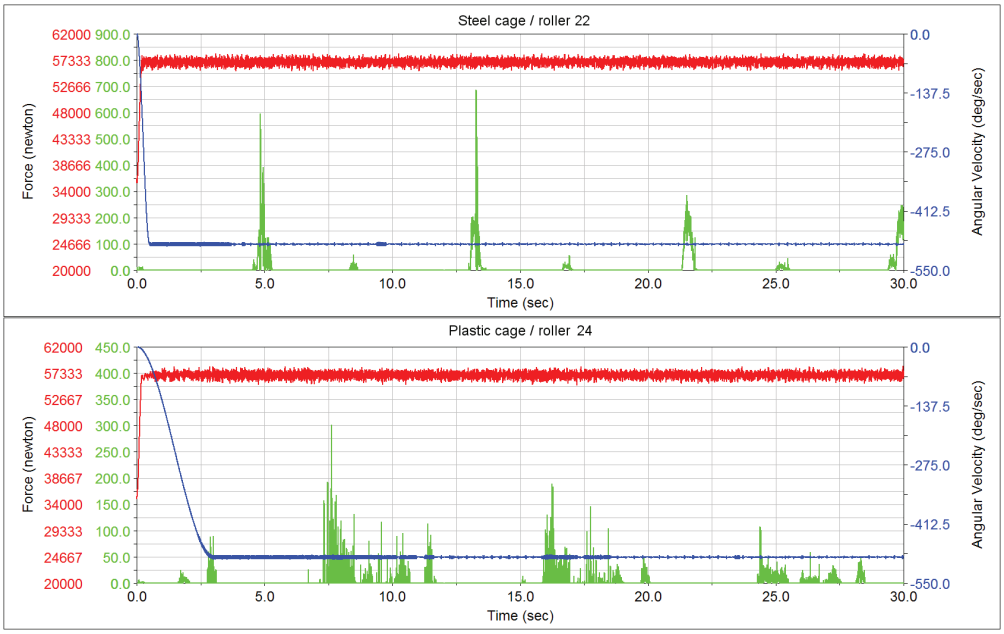

Fig. 5. *Force interaction between inner ring and rollers (red lines), force interaction between cage and rollers (green lines) and angular velocity of rollers.*

Maximum force between plastic cage and rollers was observed during interaction of the cage with roller n. 24 and is equal to 301 N (Fig. 15 down, green line). Also shown is the force between inner ring and roller n. 24 (red line), which varied between 54273 N and 58571 N. The blue line displays angular velocity of roller n. 24 and varies between 485°/s and 494°/s, similar to the velocity observed for the steel cage.

Figure 6 shows the center of gravity location in the y-z plane of steel and plastic cage, figure 7 shows force interaction between inner ring and rollers and the von Mises stress of steel cage and figure 8 shows force interaction between inner ring and rollers and the von Mises stress of plastic cage.

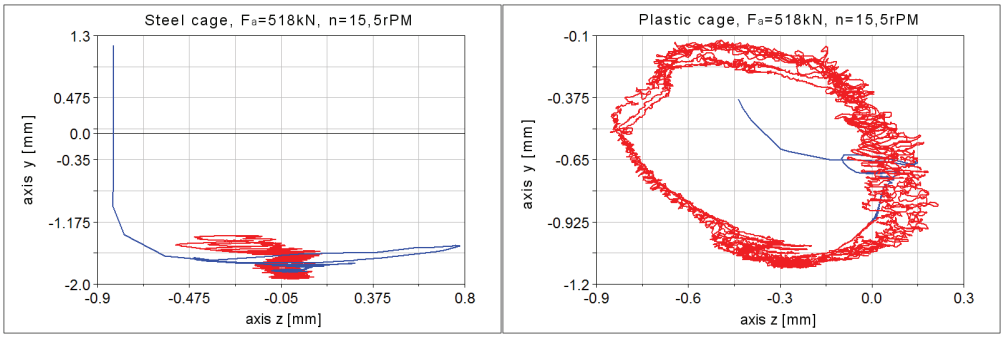

Fig. 6. *Movement of center of gravity of steel cage (left side) and plastic cage (right side) in the y-z plane under axial load*

Analysis of dynamic simulation results has shown the steel cage is in contact with rollers in lower and upper parts of the bearing, with forces in the upper bearing parts reaching up to 700 N at cage guides and 100 N at lower parts, also at cage guides. Maximum von Mises stress of 10 MPa has been recorded in time t = 2,63 s. (Fig. 7).

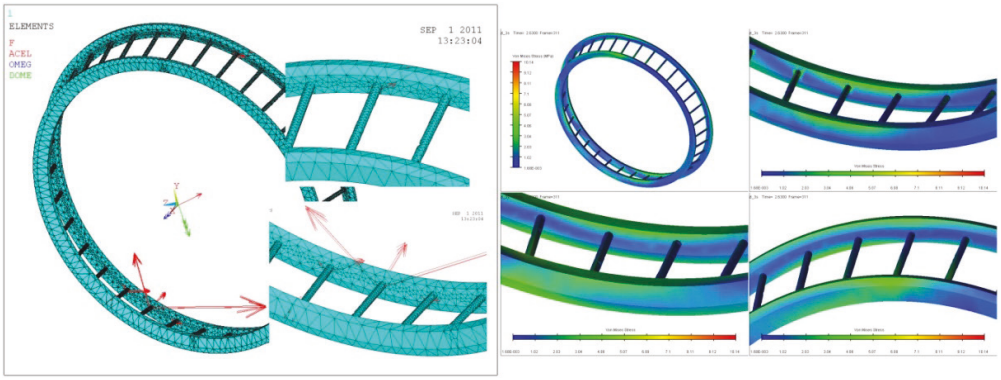

Fig. 7. *Force interaction between steel cage and rollers (left side) and maximum von Mises stress of steel cage*

Dynamic simulation of plastic cage bearing has shown similar results to those presented above. The plastic cage is in contact with rollers in lower and upper parts of the bearing. Forces in the lower part of the bearing reach up to 300 N at cage guides and up to 50 N at upper parts of the bearing cage guide surfaces. Maximum von Mises stress of 0,6 MPa has been recorded in time t = 16,8 s. (Fig. 8).

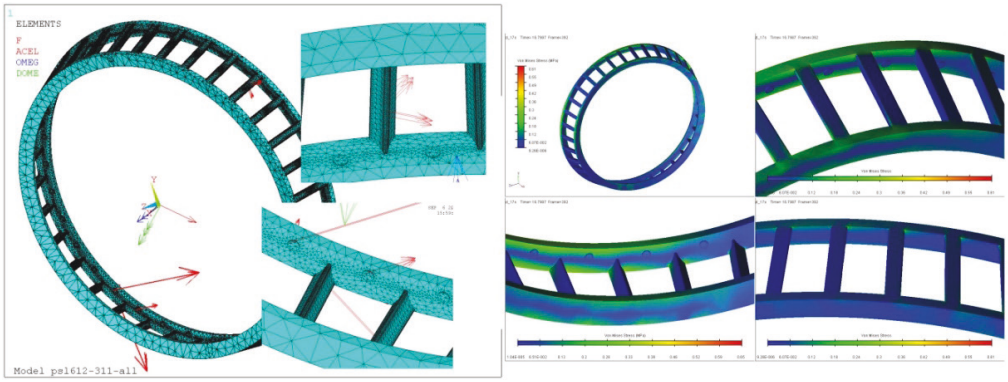

Fig. 8. *Force interaction between plastic cage and rollers (left side) and maximum von Mises stress of plastic cage*

Dynamic simulation results – radial load forces Fr=4500 kN with rotational speed n=15,5 min^{-1}

Similar to axial load force, we calculated force interactions between individual bearing parts, movement of bearing cage and angular velocity thereof when subjected to radial force.

Fig. 9 shows a comparison of load distribution of individual rollers with theoretical calculations based on [1], wherein element load Q_{max} = 56499 N. Results of the dynamic simulation have been obtained in time t = 10 seconds.

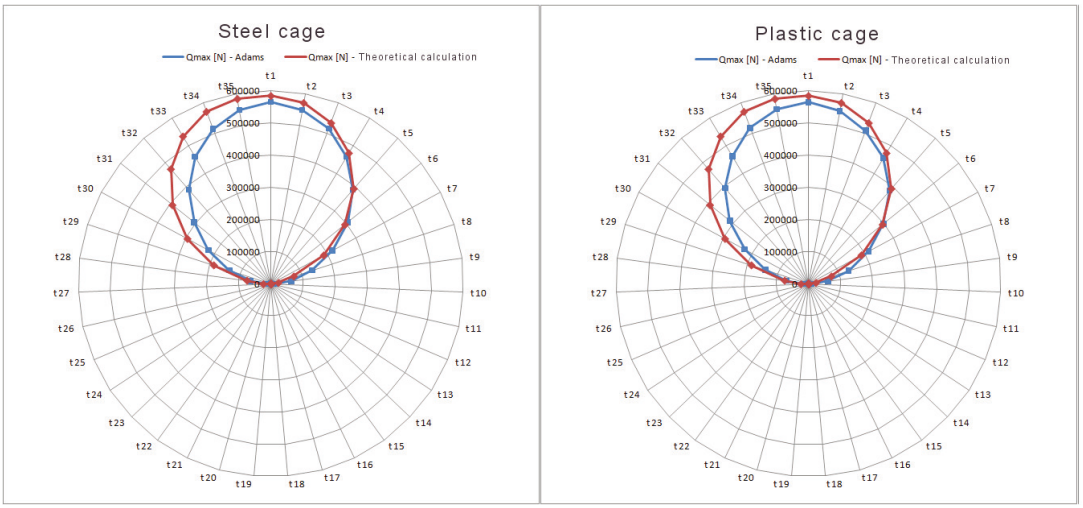

Fig. 9. *Load distribution of individual elements compared with theoretical calculations*

Figure 10 shows force between roller and cage, roller and inner ring and angular velocity of the roller. Also shown is the force between inner ring and roller n. 13 (red line). Maximum force between steel cage and rollers was observed for roller n. 13 and is equal to 800 N (green line). The analysis also showed that highest load rates are present at rollers 10 to 14 during start-up time (2-5 seconds) and are equal to 800 N. During subsequent simulation time, the cage was in contact with rollers only when the rollers were off-loaded and maximum force value was equal to 500 N. Angular speed was constant (489°/s) under applied roller load and lowered under roller load in the 20000 N to 70000 N range, achieving a minimum value of 435°/s (blue curve).

Figure 10 down shows force between inner ring and roller n. 14 (red line) for bearing with plastic cage. Maximum force between the plastic cage and rollers was observed for roller n. 14 and is equal to 691 N (green line). Similar to the steel cage, highest load rates were present at rollers 10 to 14 during start-up time (2-5 seconds) and are equal to 700 N. When compared to the steel cage, the rollers were in contact not only in the off-load phase (force equal to 150 N) but also during the load phase, with the force equal to 400 N. Angular speed was constant (489°/s) under applied roller load and, similar to the steel cage, lowered under roller load in the 20000 N to 70000 N range, achieving a minimum value of 260°/s (blue curve) and zero values under load.

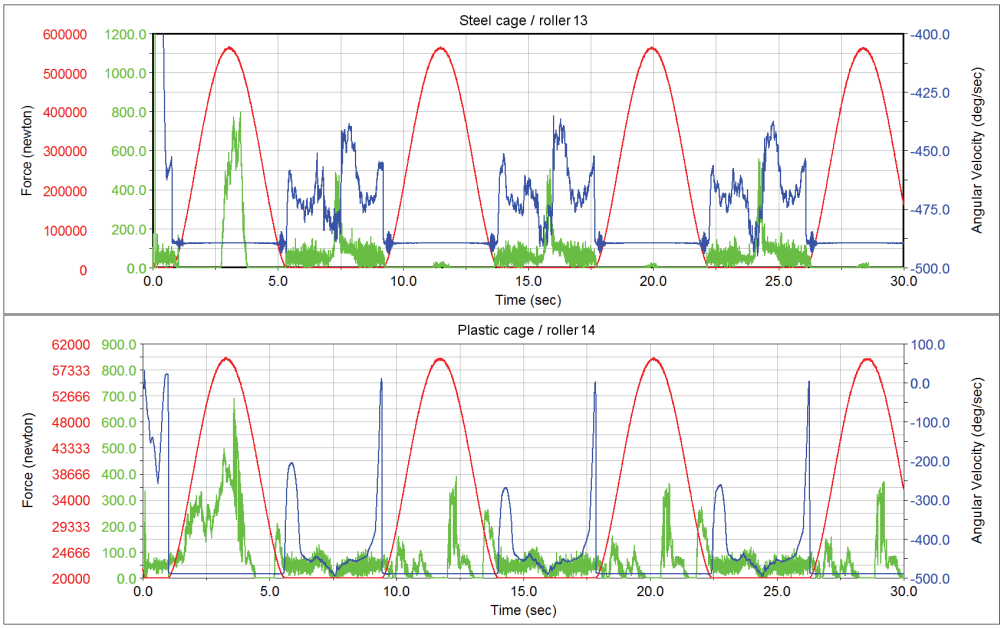

Fig. 10. *Force interaction between inner ring and rollers (red lines), force interaction between cage and rollers (green lines), angular velocity of rollers (blue line)*

Figure 11 shows the center of gravity location in the y-z plane of steel and plastic cage, figure 12 shows force interaction between inner ring and rollers and the von Mises stress of steel cage and figure 13 shows force interaction between inner ring and rollers and the von Mises stress of plastic cage.

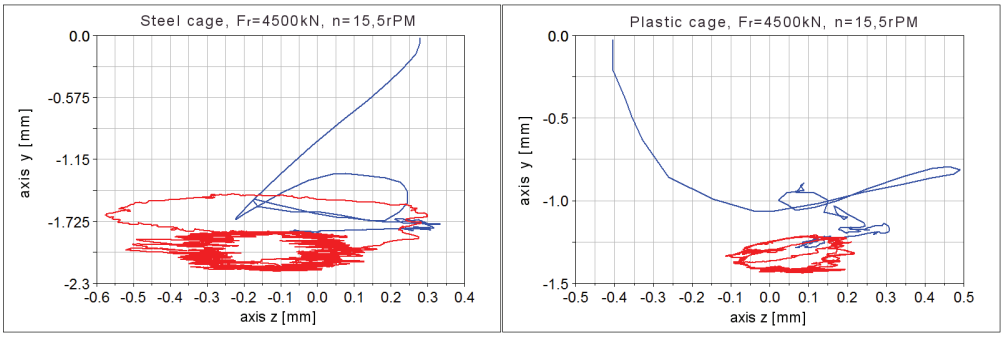

Fig. 11. *Movement of center of gravity of steel cage (left side) and plastic cage (right side) in the y-z plane under axial load*

Analysis of dynamic simulation results has shown the steel cage is in contact with rollers in lower and upper parts of the bearing, with forces in the upper bearing parts reaching up to 800 N at cage guides and 500 N at lower parts, also at cage guides. Maximum von Mises stress of 14,5 MPa has been recorded in time t = 3,5 s. (Fig. 22).

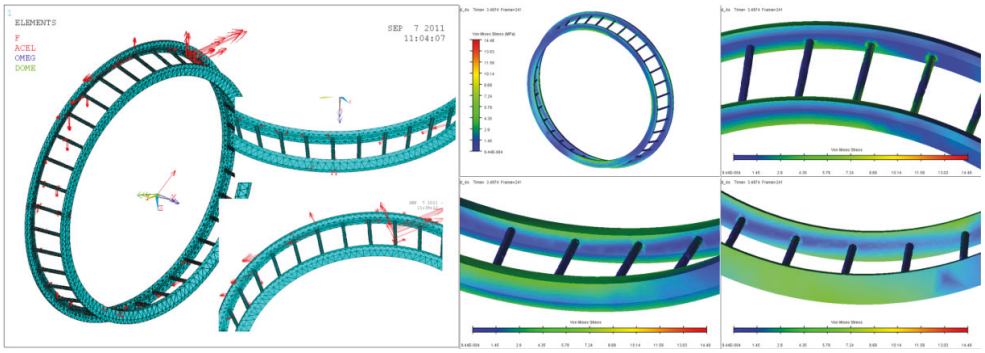

Fig. 12. *Force interaction between steel cage and rollers (left side) and maximum von Mises stress of steel cage*

Dynamic simulation of plastic cage bearing has shown similar results to those presented above. The plastic cage is in contact with rollers in lower and upper parts of the bearing. Forces in the lower part of the bearing reach up to 150 N at cage guides and up to 400 N at upper parts of the bearing cage guide surfaces. Maximum von Mises stress of 1,5 MPa has been recorded in time t = 9 s. (Fig. 13).

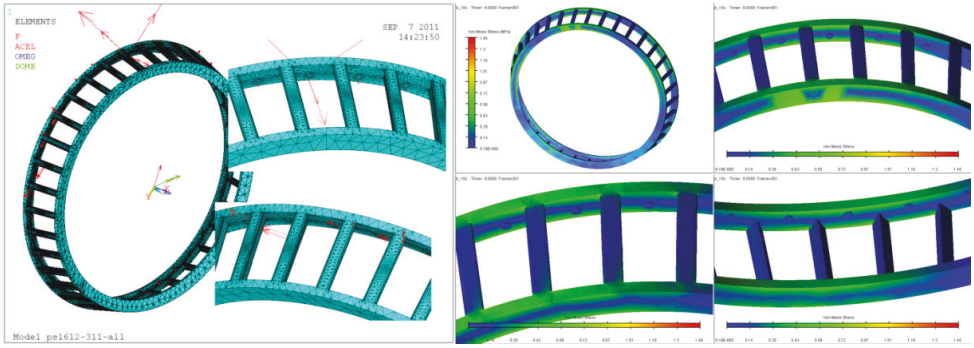

Fig. 13. *Force interaction between plastic cage and rollers (left side) and maximum von Mises stress of plastic cage*

Conclusion

Based on obtained results, we can conclude that the steel cage is more appropriate for axial force load due to lower interaction force between the cage and rollers [5, 6]. Also reduced are bearing oscillations in both the rotation axis and in the plane normal to the said axis. Forces between rollers and bearing rings are minimally influenced by the cage type. This is also true for the angular velocity of the rollers. Radial force load results in reduced load of steel cage at lower speed, however at higher speed the plastic cage is more appropriate. At lower speed, the angular velocities of bearing rollers with steel cage are randomly changing during the offload phase and could result in undesirable behavior of the bearing. Angular velocities of plastic cage rollers exhibit a smoother behavior when compared to steel cage. Additionally, oscillations in the plane normal to the rotational axis are also lowered.

Based on the afore-mentioned results, we can conclude that the use of plastic cage is more appropriate for radial load force scenarios [7, 8].

Acknowledgement

This paper presents results of work supported by the Slovak Scientific Grant Agency of the Slovak republic under the project No. VEGA 1/0077/15.

This work was supported by the Slovak Research and Development Agency under the contract No. APVV-14-0284.

References

[1] Kohár R., Medvecký Š., Hrček S. „Usage of dynamic analysis to determine force interactions between components of rolling bearings with different rotation speed". *In: Machine Design. ISSN 1821-1259. Vol. 4, No. 3*, 2012, pp. 145–150.

[2] Harris T. A., Kotzalas M. N. „*Essential Concepts of Bearing Technology*". 5. edition. 2007.

[3] Glowacz A. „Diagnostics of DC and Induction Motors Based on the Analysis of Acoustic Signals", *Measurement Science Review.* Vol. 14, No. 5, pp. 257-262, ISSN 1335-8871.

[4] Caban J., Drozdziel P., Barta D., Liscak S. „Vehicle Tire Pressure Monitoring Systems". *Diagnostyk.* Vol. 15, No. 3, 2014, ISSN 1641-6414.

[5] Drozdziel P., Komsta H., Krzywonos L. „Repair costs and the intensity of vehicle use". *Transport Problems*. Vol. 8, Issue 3, 2013, pp. 131–138.

[6] Drozdziel P., Krzywonos L. „The estimation of the reliability of the first daily diesel engine start-up during its operation in the vehicle". *Maintenance and Reliability*. 1(41)2009, pp. 4–10.

[7] Drozdziel P., Komsta H., Krzywonos L. „Repair costs and the intensity of vehicle use". *Transport Problems*. Vol. 8, Issue 3, 2013, pp. 131–138.

[8] Marczuk A., Misztal W., Słowik T., Piekarski W., Bojanowska M., Jackowska I. „Chemiczne uwarunkowania zagospodarowania elementów pojazdów poddanych recyklingowi". *Przemysl chemiczny*. 94/10(2015), pp. 1867–1871.